Applied Catalysis B: Environmental 132–133 (2013) 132–141

Contents lists available at SciVerse ScienceDirect

Applied Catalysis B: Environmental

journal homepage: www.elsevier.com/locate/apcatb

N-butanol removal over alumina supported platinum catalysts

Henri-Joël Sedjame, Gwendoline Lafaye, Jacques Barbier Jr.*

IC2MP UMR 7285 CNRS, Université de Poitiers, 4 rue Michel Brunet, 86022 Poitiers Cedex, France

ARTICLE INFO

Article history:
Received 9 July 2012
Received in revised form 24 October 2012
Accepted 23 November 2012
Available online 3 December 2012

Keywords:
Alumina
Platinum
N-butanol
Butanal
Butene
FTIR
Dehydration
Dehydrogenation
Oxidation

ABSTRACT

Pure alumina and alumina supported platinum catalysts were used in n-butanol removal reaction. Platinum catalysts were prepared by two different methods and characterized by N_2 adsorption isotherms, ICP, H_2 chemisorption and TEM. Acid–base properties of catalysts were studied by pyridine and carbon dioxide adsorption–desorption followed by FTIR. Experiments were performed by changing conditions (with or without oxygen and/or water) to determine some correlation between the reactivity and the acid–base properties of the catalysts and to study the effect of water on the reactivity. In the absence of oxygen, dehydration of n-butanol occurs whereas in the presence of oxygen the n-butanol is oxidized. In presence of oxygen, butanal is the only by-product observed whereas in absence of oxygen butene isomerization products are also observed. N-butanol dehydration involves the catalyst acidity whereas the reaction of dehydrogenation involves the basic character of the catalyst. Platinum addition changes the properties of alumina and increases the activity of catalyst for all these reactions. In large amount, water appears as an inhibitor for n-butanol oxidation.

1. Introduction

VOCs (volatile organic compounds) are known to be one of the major sources of air pollution. Thus, several studies have been made in order to eliminate these air pollutants. Noble metal catalysts based on alumina are often used for the oxidation of various VOCs [1–5]. Among the noble metals, platinum and palladium are the most popular. Papaefthimiou et al. [1] have compared several metal (Pt, Pd and Co) catalysts supported on alumina for the oxidation of three VOCs (n-butanol, benzene and ethyl acetate). Pt appears to be the most active metal for n-butanol and benzene oxidation, whereas ethyl acetate conversion is higher over cobalt catalyst. Pd activity is ten times lower than Pt for n-butanol oxidation. Alan Janbey et al. [2] have studied the influence of the support for methane oxidation. Pd is better than Pt when the used support is TiO_2. The opposite result is obtained when alumina is used as a support. Liotta [4] has shown that these differences in reactivity observed for each catalyst are related to the strength of adsorption–desorption of each VOC on various metals. It is important to point out that the adsorption–desorption of VOCs on the metal is greatly improved by the exothermic nature of the reaction and can induce some deviation in the carbon balance determination [6].

The presence and the amount of water are also important parameters that are able to modify the catalytic behavior. Generally, water acts as an inhibitor in VOC oxidation reaction [5–10], but this inhibiting character is less or more pronounced depending on other parameters. Marécot et al. have noted that water has an opposed effect on propane and propene oxidations. It depends on the composition of the used precursor to prepare Pt/alumina catalysts. When the Pt/Al_2O_3 catalysts are prepared from H_2PtCl_6, water has a promoting effect, contrary the use of $Pt(NO_2)(NH_3)_2$ salt induces an inhibiting effect of water to the hydrocarbons oxidation [5]. For the oxidation of chlorinated VOCs, water exhibits a promoting effect. Tahir and Koh have demonstrated this promoting effect for the oxidation of methylene chloride [11]. In fact, the destruction of methylene chloride without water in the feed causes catalyst deactivation and produces a significant amount of Cl_2 instead of HCl whereas in presence of water the catalyst performance is stabilized thereby producing the desired HCl rather than Cl_2. The recent studies are generally focused on applied research, however, in the past, several fundamental studies have been made on alumina to study its physico-chemical properties and the reactivity resulting [12–21].

Alumina has been well known as a bifunctional oxide having basic and acidic sites [12]. Surface acidity is usually attributed to Al^{3+} ions (Lewis acidity), while basicity is linked to the number of oxygen ions O^{2-} (Lewis basicity). Hydroxyl groups are both acidic (Brønsted acidity) and basic sites [12,14,15]. It has been demonstrated that the surface acidity depends on the activation

* Corresponding author. Tel.: +33 549 45 48 31; fax: +33 549 45 34 99.
E-mail address: jacques.barbier.jr@univ-poitiers.fr (J. Barbier Jr.).

0926-3373/$ – see front matter © 2012 Elsevier B.V. All rights reserved.
http://dx.doi.org/10.1016/j.apcatb.2012.11.032

Table 1
Characterizations of the catalysts.

	SBET ($m^2\ g^{-1}$)	Average pore size (Å)	Pt loading (wt%)	Dispersion (%)
γ-Al_2O_3	100	183	n.a.	n.a.
Pt/γ-Al_2O_3	100	185	0.2	77
Pt/Al_2O_3-one-pot	400	31	0.2	54

temperature [16,17] in accordance with the formation of acidic sites, Al^{3+}, while Yamadaya et al. have proved that basicity increases with hydration and remains constant when the amount of adsorbed water corresponds to three molecular layers [20]. Carbon dioxide adsorption followed by FTIR [21] showed (i) that the strongest basicity is attributed to oxygen ions near to hydroxyl groups and (ii) that the basicity decreases when dehydroxylation increases. Berteau et al. [13] have showed that these acid–base properties can be modified by the addition of anions or cations. Thus γ-Al_2O_3/Na^+ presents the lowest acidity and γ-Al_2O_3/F^- presents the lowest basicity. Bailey and Wightman [22] have concluded from a study of vapor adsorption on α-Al_2O_3 and γ-Al_2O_3 at 30, 40 and 50 °C that water adsorption decreases with the increase of temperature. Experiments of water vapor readsorption after desorption show that water adsorption on alumina is fully reversible. They have concluded that water adsorption on alumina is a physisorption process. According to several authors, the activity of alumina is closely related to the acid sites created during desorption of water from the surface [23–26]. These sites appear to be Al^{3+} ions [15,26].

Since the efficiency of Pt/γ-Al_2O_3 has been proved by several authors [1–5] for oxidation of non-halogenated VOCs such as n-hexane, methanol, n-butyl-amine, toluene, propane and propene, the aim of this work is to correlate the activity of catalysts based on alumina for the different reactions occurring during the elimination of n-butanol (dehydrogenation, dehydration and oxidation) with their acid–base properties determined by FTIR study. Effects of water and method of catalyst preparation on these reactions are also investigated.

2. Experimental

2.1. Catalyst preparation

The catalysts tested in this work were γ-Al_2O_3 and two Pt/γ-Al_2O_3 catalysts. γ-Al_2O_3 provided by Rhodia (EC 12/347/87) was sieved and calcined at 500 °C in air (80% nitrogen, 20% oxygen) for 4 h. The catalysts based on platinum were prepared by two different methods. The first method (method 1) is an incipient wetness impregnation of γ-Al_2O_3 with an aqueous solution of $Pt(NH_3)_4(OH)_2$ (8–11% Pt). 5.5 g of γ-Al_2O_3 was added to 103.4 mg of the $Pt(NH_3)_4(OH)_2$ solution. The mixture was stirred (300 rpm) overnight. The catalyst (Pt/γ-Al_2O_3) was then dried at 50 °C for 18 h, calcined in air at 400 °C for 4 h and reduced in hydrogen at 300 °C for 4 h. The heating ramp was 10 °C min^{-1}. The second method (method 2) is based on a sol–gel process: the noble metal precursor is added directly in the preparation of the alumina. 5 g of Pluronic P123 was dissolved in 100 ml of ethanol and stirred at ambient temperature for 1 h. 5.2 g of citric acid, 10.3 g of aluminum isopropoxide and 10.85 mg of $Pt(acac)_2$ were added into the solution above. The mixture was stirred at ambient temperature for 5 h and dried in an oven (60 °C) for 5 days. The catalyst (Pt/Al_2O_3-one-pot) was calcined in air at 400 °C for 4 h. This second method was inspired by the literature [27]. Prior to use, the three catalysts (γ-Al_2O_3, Pt/γ-Al_2O_3 Pt/Al_2O_3-one-pot) were sieved to retain particles with sizes between 0.25 and 0.40 mm. The elemental analysis of the platinum was determined by ICP. The Pt loading of Pt/γ-Al_2O_3 and Pt/Al_2O_3-one-pot is equal to 0.2 wt%.

2.2. Catalyst characterization

The BET specific surface areas were measured by nitrogen physisorption at −195.8 °C using a Micromeritics Tristar apparatus. The BJH method was used to determine the mean pore size. Samples were previously degassed at 250 °C under high vacuum (0.1–0.2 mbar) overnight.

The Pt loading was measured by Inductively Coupled Plasma (ICP) using a Perkin-Elmer Optima 2000 DV apparatus. Before analysis, a known mass of powder was dissolved in acid under microwave heating.

The metal dispersion was measured by hydrogen chemisorption in a chromatographic microreactor at ambient temperature. Hydrogen pulses (0.25 ml) were injected in regular intervals after reduction under H_2 (300 °C, 1 h).

TEM measurements were carried out on a Jeol JEM 2100 equipped with a LaB6 filament. The apparatus has a linear resolution of 0.14 nm and is equipped with a Gatan Ultrascan CCD camera with a resolution of 2k × 2k. Before analysis, powder was dispersed in ethanol, and the solution dropped on a copper grid.

The surface hydroxyl groups are identified by FTIR (Fourier Transformed InfraRed) spectroscopy (Thermo Nicolet 5700). Samples were compacted into thin pellets and activated at 500 °C under a secondary vacuum (10^{-6} mbar) overnight. After cooling until ambient temperature, a spectrum was recorded to identify hydroxyl groups on the sample surface. The catalyst acidity was characterized by pyridine adsorption followed by FTIR spectroscopy (Nexus Nicolet 5700). Samples were compacted into thin pellets and activated at 450 °C under a secondary vacuum (10^{-6} mbar) overnight. After cooling until ambient temperature, pyridine adsorption was performed for 5 min after pressure stabilization. The cell was then kept under a secondary vacuum for 1 h. The thermodesorption of pyridine was carried out at different temperatures from 50 °C to 450 °C with a temperature step of 50 °C. The IR spectra were recorded at ambient temperature in a spectrometer equipped with a DTGS detector (Deuterium TriGlyceride Sulfur) and KBr beam splitter, with a resolution of 2 cm^{-1} and 64 scans. Table 1 shows the characteristics of the catalysts tested in this work.

2.3. Catalytic experiments

The gaseous feed used for the catalytic tests was composed of 1000 ppmv of n-butanol in synthetic air. Different amounts of water (0, 3 and 10%) were added to the feed in order to increase the relative humidity of the air and to evaluate the effect of water on the catalytic reaction. N-butanol and water were heated in two thermostated and pressurized (5 bar) saturators. An accurate flow of nitrogen was bubbled through these saturators and the outflow was mixed with the synthetic air ($N_2 + O_2$) in order to obtain 0, 3 or 10% of H_2O and 0.1% of n-butanol in the feed at the reactor inlet. For the tests without oxygen (t1 and t3, Table 4), the synthetic air was replaced by nitrogen. Transfer lines were heated at 110 °C to avoid condensation. Mass flow and temperature controllers were Brooks instruments 0254. The total flow rate was kept constant for all experiments (70 ml min^{-1}). Reactions were carried out in a tubular fixed bed reactor placed in an electrical

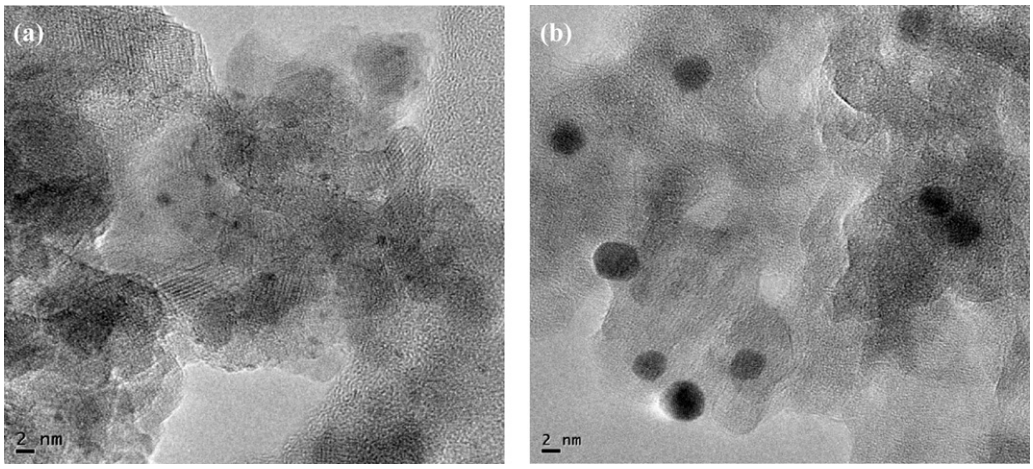

Fig. 1. HRTEM images of (a) Pt/Al_2O_3 and (b) Pt/Al_2O_3-one-pot.

furnace equipped with a temperature programmer. A thermocouple was inserted in the reactor, embedded in the catalyst bed to measure exactly the reaction temperature. 140 mg of catalyst mixed with 1 g of cordierite were used for the reactions. Catalysts and cordierite have the same grain size ($0.25 < d < 0.4$ mm). The space velocity was estimated at 60,000 h^{-1}. The reaction products were analyzed by a Gas Chromatograph (Varian 490-GC) equipped with a thermal conductivity detector (TCD) and two columns: a Porapak Q (PPQ) to analyze air and carbon dioxide and a CP sil-5CB to analyze hydrocarbons (n-butanol, butanal, butene, etc.). Experiments were performed between 40 and 350 °C and the temperature was increased linearly by 0.5 °C min^{-1}. The accuracy on the results is about ±1 °C. It is important to notice that n-butanol adsorption is observed when the catalytic test begins: the n-butanol amount at the reactor outlet increases slowly until it reaches ~1000 ppmv. This adsorption is more or less important depending on the catalyst and is compensated by a desorption occurring at higher temperatures (the adsorption corresponds to a carbon balance <100% and the desorption to a carbon balance higher than 100%). Therefore, the conversion curves presented in this paper begin when adsorption is no longer visible, that is 50 °C.

The following results are expressed in terms of %:

- N-butanol molar percent = $100 \times ([C_4H_9OH]/[C_4H_9OH]_{in})$
- Butanal yield = $100 \times ([C_4H_8O]/[C_4H_9OH]_{in})$
- Carbon dioxide yield = $100 \times ([CO_2]/(4 \times [C_4H_9OH]_{in}))$
- Yield of butenes = $100 \times (([1\text{-}C_4H_8] + [2\text{-trans-}C_4H_8] + [2\text{-cis-}C_4H_8])/[C_4H_9OH]_{in})$
- Butene isomerization = $100 \times (([2\text{-trans-}C_4H_8] + [2\text{-cis-}C_4H_8])/([1\text{-}C_4H_8] + [2\text{-trans-}C_4H_8] + [2\text{-cis-}C_4H_8]))$
- Carbon balance = $100 \times (((\sum[C_4] + [CO_2])/4)/[C_4H_9OH]_{in})$
- Selectivity to carbon dioxide = $100 \times [CO_2]/([CO_2] + [C_4H_8O] + [1\text{-}C_4H_8] + [2\text{-trans-}C_4H_8] + [2\text{-cis-}C_4H_8])$

where $[C_4H_9OH]_{in}$ is the inlet concentration of n-butanol, $[C_4H_9OH]$, $[C_4H_8O]$, $[CO_2]$, $[1\text{-}C_4H_8]$, $[2\text{-trans-}C_4H_8]$ and $[2\text{-cis-}C_4H_8]$ are the outlet concentrations of n-butanol, butanal, carbon dioxide, 1-butene, 2-trans-butene and 2-cis butene respectively and $\sum[C_4]$ is the sum of outlet concentrations of hydrocarbons containing four carbons.

3. Results and discussion

3.1. Catalyst characterization

The main characteristics of $\gamma\text{-}Al_2O_3$, $Pt/\gamma\text{-}Al_2O_3$ and Pt/Al_2O_3-one-pot catalysts are summarized in Table 1. No appreciable change in specific surface area and pore size can be observed after impregnation of Pt salt on $\gamma\text{-}Al_2O_3$. On the other hand, monometallic Pt catalyst prepared by sol–gel procedure allows achieving largely higher surface area (400 $m^2\,g^{-1}$). Nevertheless, the dispersion of Pt/Al_2O_3-one-pot is lower than the one of $Pt/\gamma\text{-}Al_2O_3$. The comparison of the high resolution transmission electron microscopy (HRTEM) images (Fig. 1) shows that the metal particle size is larger for Pt/Al_2O_3-one-pot. This observation proves that the lower metallic accessibility of the sol–gel derived catalyst is mainly due to a higher average particle size and not due to an encapsulation phenomenon of Pt particles in Al_2O_3 occurring during the sol–gel preparation as it could be suspected.

The three materials $\gamma\text{-}Al_2O_3$, $Pt/\gamma\text{-}Al_2O_3$ and Pt/Al_2O_3-one-pot were analyzed by FTIR to characterize the free hydroxyl groups on the alumina surface. Each hydroxyl has its own vibration frequency, in the 3900–3500 cm^{-1} region, depending to its mode of coordination to the aluminum atom. In the literature, Knözinger et al. [15], Tsyganenko et al. [28] and Digne et al. [29] have established a relation between the vibration frequency υ(OH) and the acid–base properties of hydroxyl. These assignments are

Table 2
OH assignment on the alumina surface.

Scheme		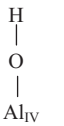	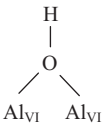	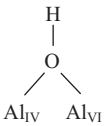	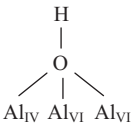
Type of OH	Ib	Ia	IIb	IIa	III
υ(OH) (cm^{-1})	3800–3785	3780–3760	3758	3735–3730	3710–3690
Charge	−0.5	−0.25	0	0.25	0.5
Acidity	−−	−	0	+	++

Table 3
Amount of the Lewis acid sites (LAS) on the catalysts.

Catalyst	Total LAS (μmol g^{-1})	Strong LAS (μmol g^{-1})	Medium LAS (μmol g^{-1})
γ-Al_2O_3	150	35	115
Pt/γ-Al_2O_3	150	50	100
Pt/Al_2O_3-one-pot	183	50	133

Table 4
Conditions of catalytic tests performed on γ-Al_2O_3 and Pt/γ-Al_2O_3 (1000 ppmv n-butanol, total flow rate 70 mL/min) and T_{50} and T_{90} of γ-Al_2O_3 and Pt/γ-Al_2O_3 for the catalytic tests t1, t2, t3 and t4.

Test	Conditions	Code names	γ-Al_2O_3		Pt/γ-Al_2O_3	
			T_{50} (°C)	T_{90} (°C)	T_{50} (°C)	T_{90} (°C)
t1	No water, no oxygen	No H_2O, no O_2	266	295	185	220
t2	With oxygen only	O_2	150	180	105	148
t3	With 3% of water only	3% H_2O	283	310	179	210
t4	With oxygen and 3% of water	O_2–3% H_2O	160	190	103	147
t5	With oxygen and 10% of water	O_2–10% H_2O	n.a	n.a	n.a	n.a

summarized in Table 2. Type I hydroxyls present the highest basicity and Type III hydroxyls the highest acidity.

The OH stretching region for the different catalysts activated under vacuum at 500 °C is presented in Fig. 2. The IR spectra of γ-Al_2O_3 and Pt/γ-Al_2O_3 are consistent with those reported in the literature [28,29] showing the five different OH types of alumina. Using Table 2, the bands can be assigned to isolated OH groups of Type I (most basic OH group, 3788 and 3773 cm^{-1}), Type IIb (3753 cm^{-1}), Type IIa (3728 cm^{-1}) and Type III (most acidic OH group, 3681 cm^{-1}). The IR spectrum of Pt/Al_2O_3-one-pot is less defined than γ-Al_2O_3, Pt/γ-Al_2O_3. The Type I hydroxyls peaks are merged into a broad peak at 3780 cm^{-1}, the Type IIb hydroxyl peak does not appear and the Type IIa hydroxyl peak appears at 3730 cm^{-1}. The peak of the most acidic hydroxyl group is lower than that of γ-Al_2O_3 and Pt/γ-Al_2O_3 but appears at the same wave number. Pt/Al_2O_3-one-pot presents Type I hydroxyls peak more intense than γ-Al_2O_3 and Pt/γ-Al_2O_3. This observation suggests that it possesses more basic hydroxyl groups than Pt/γ-Al_2O_3 and γ-Al_2O_3.

The acidic properties of the three materials were probed with pyridine adsorption followed by FTIR. This technique allows a clear distinction between Brønsted and Lewis acid sites. No IR band assigned to pyridinium ions (PyH^+) was observed, as expected on alumina which does not present OH groups strong enough to protonate the pyridine. Only bands assigned to coordinated pyridine on Lewis acid sites (LAS) were observed. According to the literature, the bands distinguished at 1625 and 1620 cm^{-1} are assigned to coordinated pyridine to tetrahedral Al^{3+} (strong LAS) and to both

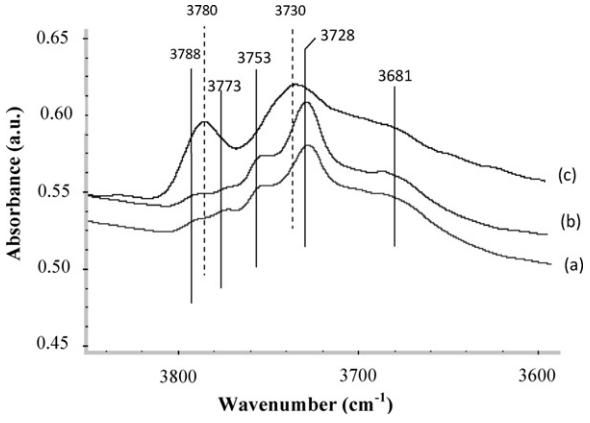

Fig. 2. IR spectra at the υ(OH) region for (a) γ-Al_2O_3, (b) Pt/γ-Al_2O_3 and (c) Pt/Al_2O_3-one-pot catalysts outgassed at 500 °C.

tetrahedral and octahedral Al^{3+} (medium to weak LAS) [30,31]. The area of the ν19b band at 1451 cm^{-1} is used to quantify the total amount of LAS, using its molar adsorption coefficient (ε = 1.5 cm μmol^{-1} [32]). The total amount of LAS was measured using the area of the ν19b band after evacuation at 150 °C whereas the strongest LAS was determined considering this band after evacuation at 300 °C [33]. The results of this study are reported in Table 3. The impregnation of Pt salt on γ-Al_2O_3 has no significant effect on the total number of LAS but on the distribution between medium and strong LAS. Indeed, the presence of Pt increases the amount of strong LAS by ~15 μmol g^{-1} (Table 3), which is consistent with the Pt loading (~10 μmol g^{-1}). The distribution between medium and strong Lewis acid sites can be influenced by the nature of the platinum/support bond. The coordination of the aluminum atom can indeed be modified and its acid–base properties can be changed consequently. The Pt/Al_2O_3-one-pot exhibits the highest amount of LAS but Pt/γ-Al_2O_3 presents the highest amount of strong LAS.

The overall FTIR study has demonstrated that hydroxyl groups and Lewis acid sites distribution deviate between the different samples. These observed differences in terms of surface acid–base properties could affect the catalysts activity for n-butanol removal.

3.2. Catalytic removal of n-butanol on γ-Al_2O_3 and Pt/γ-Al_2O_3: study of various parameters

Five sets of catalytic tests were performed on γ-Al_2O_3 and Pt/γ-Al_2O_3 with changes in operating conditions. The five sets of experiments differ depending on the presence or the absence of oxygen and/or water, with the aim of proposing mechanisms of reactions taking place on the catalyst surface. The operating conditions of these tests and their code names are listed in Table 4. For all the tests, Fig. 3 and Fig. 4 display the concentration profiles of the reactant and the main products with reaction temperature during n-butanol removal on γ-Al_2O_3 and Pt/γ-Al_2O_3, respectively. It is important to point out that n-butanol was found to react without catalyst in air and in nitrogen. However, in presence or in absence of oxygen, butanol starts to be converted at temperatures above 190 °C and is completely destructed at ~270 °C in presence of oxygen and at T > 350 °C without oxygen.

3.3. Influence of platinum

The aim of this study was to investigate the changes in catalytic properties of alumina in n-butanol removal when Pt is added on alumina surface. For all the tests, the comparison of the results obtained over γ-Al_2O_3 (Fig. 3) and over Pt/γ-Al_2O_3 (Fig. 4), reveals that the temperature of appearance of butanal depends on the

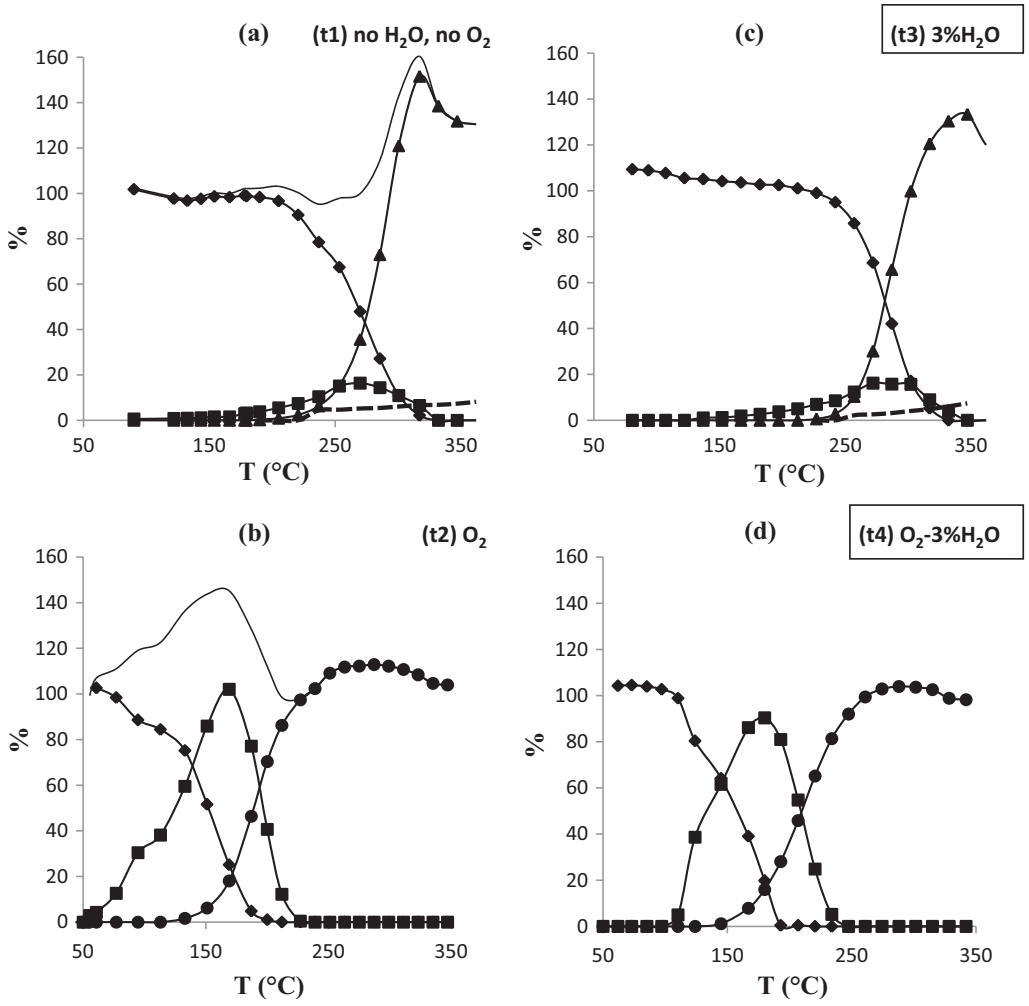

Fig. 3. Results obtained from the removal of n-butanol over γ-Al_2O_3 for (a) test1, (b) test2, (c) test3 and (d) test4: (♦) n-butanol, (■) butanal, (▲) butenes, (●) carbon dioxide, (- - -) butene isomerization and (—) carbon balance.

operating conditions in the case of γ-Al_2O_3, whereas in the presence of platinum, butanal formation always starts around 55 °C, which is from the beginning of the experiments. This improvement of the catalytic activity due to the presence of platinum can also be observed from the n-butanol conversion profiles with the temperature. For instance, for the test 1 (no O_2–no H_2O), the comparison of Fig. 3(a) and Fig. 4(a) shows that in the presence of platinum, the temperature required to obtain the same conversion of n-butanol (T_{50}) into butanal and butene is reduced by ~80 °C. Likewise for test 2 (O_2), the temperature required for the same conversion of n-butanol (T_{50}) is diminished by ~50 °C (Table 4). Similar high catalytic activity of platinum for alcohol dehydrogenation and oxidation has already been reported in the literature [1,34,35].

It should be noticed that a phenomenon of isomerization of 1-butene occurs when the reaction is performed in the absence of oxygen (tests 1 and 3). Fig. 4(a) shows that on Pt/γ-Al_2O_3 the isomerization starts around 150 °C, reaches 80% and then drops to 15% at higher temperature. This phenomenon is less important at high temperature (~250 °C) for the reason that 1-butene desorbs more easily. In the presence of γ-Al_2O_3, isomerization starts around 220 °C and reaches only 8% (Fig. 3(a)). It clearly appears that the addition of platinum to γ-Al_2O_3 promotes 1-butene isomerization. According to Van Roosmalen et al. [36], the isomerization of butene is closely related to the content of Al^{3+} ions. This assumption is confirmed by Ballivet et al. [37] who have demonstrated that the catalytic activity decreases when Al^{3+} ions are removed by acid leaching. The studies of Knözinger [15] and Peri [26] showed that these Al^{3+} ions would be generated by a dehydroxylation of alumina. Since the number of strong LAS increases in presence of platinum (Table 3), the addition of platinum can be responsible for the promotion of 1-butene isomerization.

3.4. Influence of oxygen

For both catalysts, in the presence of oxygen, there is no butene formation and butanal turns into carbon dioxide. Moreover, the temperature required to totally convert n-butanol is lowered by 120 °C in the presence of oxygen.

Fig. 3(a) and Fig. 4(a) reveal that the formation of butanal on γ-Al_2O_3 and Pt/γ-Al_2O_3 is possible in the absence of oxygen, but Fig. 3(b) and Fig. 4(b) demonstrate that oxygen promotes highly this reaction. Thus, on γ-Al_2O_3, in the presence of oxygen, butanal is formed faster and in large quantities between 54 and 224 °C (Fig. 3(b)). The carbon balance over 100% between 55 and 212 °C corresponds to the n-butanol desorption in the form of butanal (Fig. 3(b)). In the absence of oxygen, butanal is formed in small quantity (between 90 and 332 °C) and reaches its maximum value (corresponding to a n-butanol conversion <20%) at 269 °C (Fig. 3(a)). Carbon balance is once again over 100%, but at higher temperature (from 270 °C) and corresponds to 1-butene formation. Similar

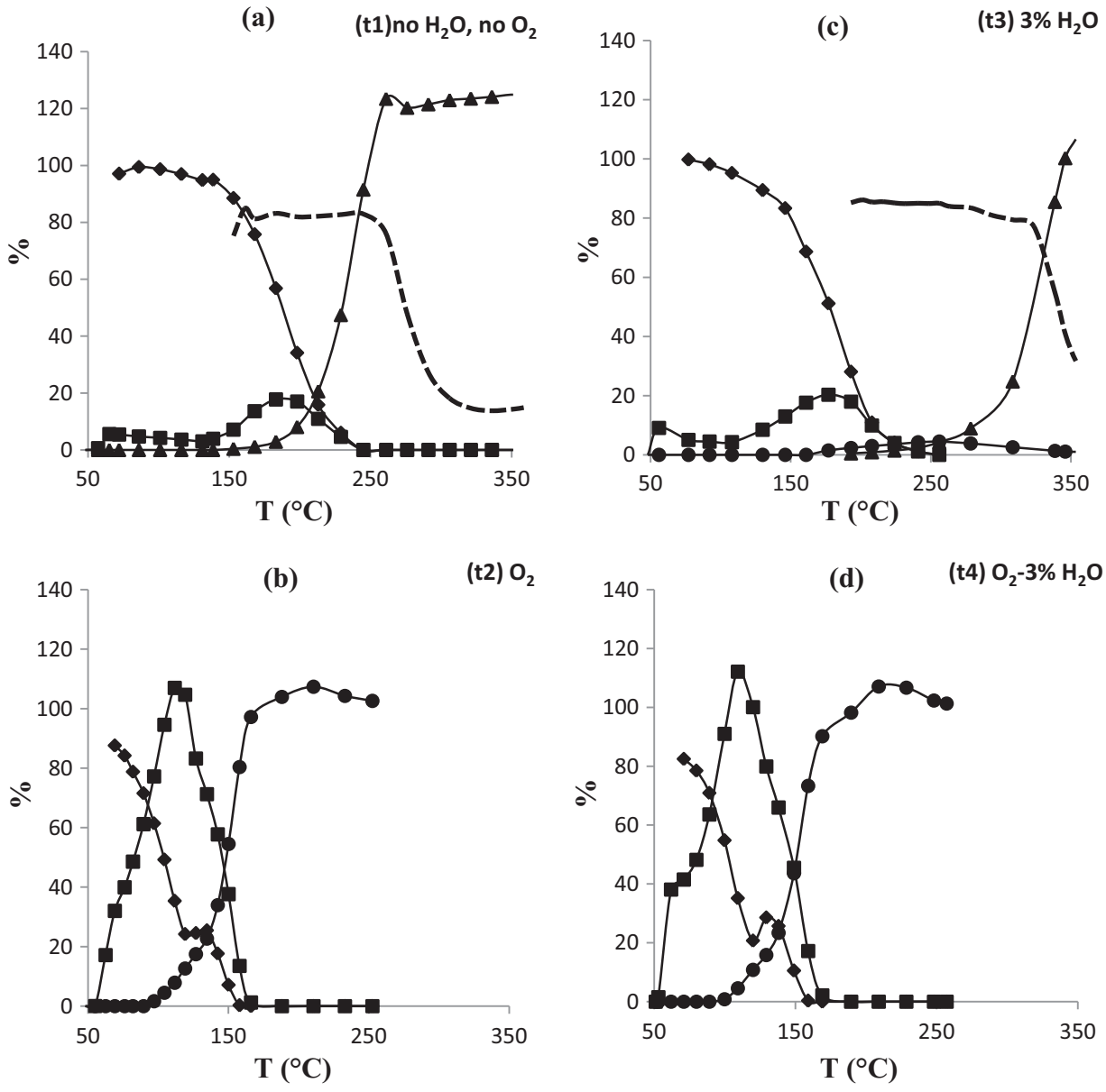

Fig. 4. Results obtained from the removal of n-butanol over Pt/γ-Al_2O_3 for (a) test1, (b) test2, (c) test3 and (d) test4: (♦) n-butanol, (■) butanal, (▲) butenes, (●) carbon dioxide, and (- - -) butene isomerization.

results were obtained on Pt/γ-Al_2O_3 except that the reactions occur at lower temperatures: ∼50 °C lower with oxygen (Fig. 4(b)) and ∼90 °C lower in the absence of oxygen ((Fig. 4(a)).

In the absence of oxygen, the products of reactions on γ-Al_2O_3 and Pt/γ-Al_2O_3 are butanal, 1-butene and water. The above results suggest that butanal and butene are formed in parallel:

butanal ← n-butanol → 1-butene

Moreover, the formation of these products on pure alumina can be attributed exclusively to basic and acid sites of alumina, these sites being activated by heating. Fig. 5 proposes mechanism for these reactions. According to the proposed mechanism, butanal formation would proceed via the adsorption of n-butanol on a Lewis acid site by the oxygen electronic doublet of the alcohol function and on a basic site by the hydrogen from the hydroxyl group. These adsorption steps would be followed by H-atom abstraction from the α carbon atom by a weak basic site (Fig. 5(a)) leading to the formation of butanal and H_2. Likewise for the formation of butene, except that for this mechanism the abstraction of H-atom is from the β carbon atom by a strong basic site (Fig. 5(b)).

In the presence of oxygen, there is no butene formation and butanal turns into carbon dioxide. The reaction of n-butanol oxidation appears to be successive in accordance with the literature [1,34]:

n-butanol → butanal → CO_2

It takes place at low temperature (<150 °C), that is before the activation of the basic sites, responsible of the abstraction of H-atom leading to butanal and butene formation in absence of oxygen. These sites are therefore not implicated in the reaction. This result signifies that oxygen is involved in the reaction: (i) on γ-Al_2O_3, oxygen in the gas phase reacts with n-butanol adsorbed on the catalyst by the mechanism of Eley-Rideal, (ii) on Pt/γ-Al_2O_3, both reactants are adsorbed on the catalyst, the reaction occurs by a mechanism of Langmuir–Hinshelwood. Similar mechanisms have been proposed for VOCs by Abbasi et al. [38]. Moreover, for both

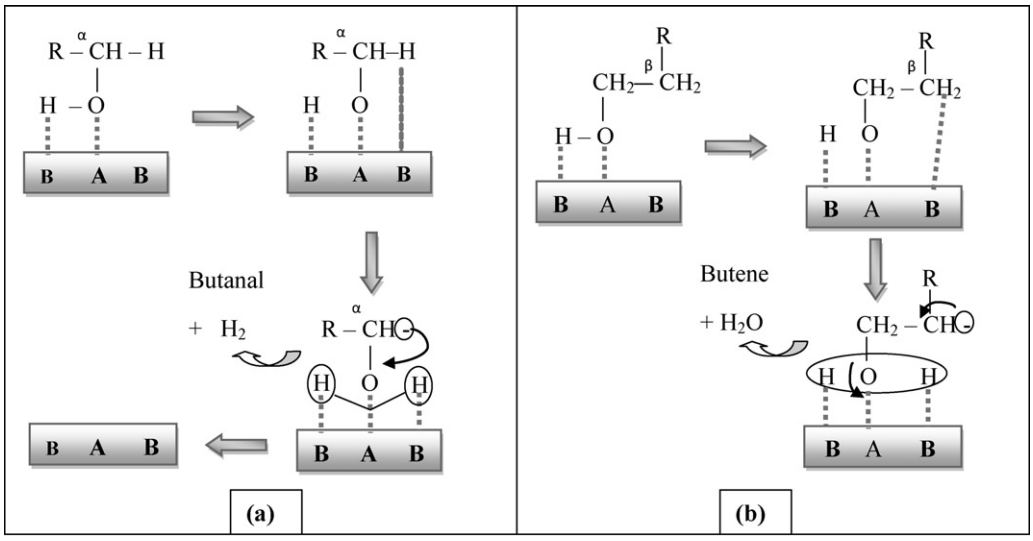

Fig. 5. Proposed mechanisms of butanal and butene formation over alumina.

samples, the temperature required to totally convert n-butanol is lowered by 120 °C in the presence of oxygen.

3.5. Influence of water

Water is known to adsorb onto alumina and increase its basicity [22]. Therefore, it could be conceived, at high temperature, a balance between dehydroxylation and hydration, affecting products formation.

On γ-Al_2O_3, in the presence and in the absence of oxygen, water has no significant effect on the quantity of the products, but delays their formation. An example can be given for test 2 and test 4 (O_2 and O_2–3%H_2O respectively); Fig. 3(b) and (d) corresponding to these tests show that the temperatures required to start butanal and carbon dioxide formation are increased by ~50 °C and ~15 °C, respectively, in the presence of water. At low temperature (<100 °C), an adsorption competition between water and n-butanol could be the cause of the delay in the formation of butanal. In order to verify this assumption, the n-butanol adsorption capacity of γ-Al_2O_3 in the presence and in the absence of water was evaluated. N-butanol was adsorbed in the presence and in the absence of water on γ-Al_2O_3 samples previously calcined at 500 °C for 4 h. The resulting samples were then treated in TGA–DSC to determine the loss of mass corresponding to the amount of hydrocarbon adsorbed on the catalysts. It appears that the sample treated with water has adsorbed less n-butanol than its counterpart treated without water (mass loss = 3.12 wt% versus 4.50 wt%). This result is in accordance with the assumption of an adsorption competition between n-butanol and water. At high temperature, there is no significant effect of water on the total conversion of n-butanol but an impact on butanal formation and oxidation toward carbon dioxide.

On Pt/γ-Al_2O_3, the adsorption competition between water and n-butanol exists probably, but has no visible effect on butanal formation for the reason that the catalyst is very active. Thus, butanal formation starts around 55 °C, whatever the amount of water in the reaction medium.

In the absence of oxygen, with and without water (test3 and test1, respectively), the high proportion of water (not presented in the figures) formed during the course of reaction on Pt/γ-Al_2O_3 can be explained by butene formation. In presence of water (Fig. 4(c)), a formation of carbon dioxide is detected before butene appearance. This carbon dioxide formation can be attributed to a steam reforming of butene adsorbed on the catalyst, following the equation:

$$C_xH_y + 2xH_2O \rightarrow xCO_2 + (2x + 1/2y)H_2$$

Indeed, several authors have shown the activity of platinum for hydrocarbon steam reforming reactions [39,40]. Moreover, the FTIR study shows that the number of strong LAS, responsible sites for water activation in steam reforming reaction, increases in the presence of platinum. In Fig. 6, a mechanism of this reaction is proposed: water is activated by the support and forms an intermediate with butene adsorbed on the metal; then the dissociation takes place on the metal leading to carbon dioxide. At higher temperature, carbon dioxide formation decreases, because butene desorbs before the steam reforming occurs.

Fig. 7 shows the selectivity to carbon dioxide for γ-Al_2O_3 and Pt/γ-Al_2O_3 in the presence of oxygen with 0, 3 and 10% of water (t2, t4 and t5 respectively) as a function of n-butanol conversion (T_x: temperature for a n-butanol conversion = x%). It can be noted that the selectivity to carbon dioxide decreases with the amount of water. Thus, generally, in the presence of oxygen, water inhibits the total oxidation of n-butanol.

3.6. Effect of the preparation method of Pt catalysts

The above results dealt with a Pt catalyst prepared by incipient wetness impregnation. A comparison was made with a sol–gel derived Pt catalyst, named Pt/Al_2O_3-one-pot. It should be noted that HRTEM analysis indicates no structural changes on the catalysts after n-butanol removal reaction.

Fig. 8 shows the n-butanol consumption (Fig. 8(a)), butanal and carbon dioxide formation (Fig. 8(b) and Fig. 8(c)) and carbon balance (Fig. 8(d)) as function of the temperature for the reaction of n-butanol oxidation in presence of 3% of water. Pt/Al_2O_3-one-pot appears to be more active than

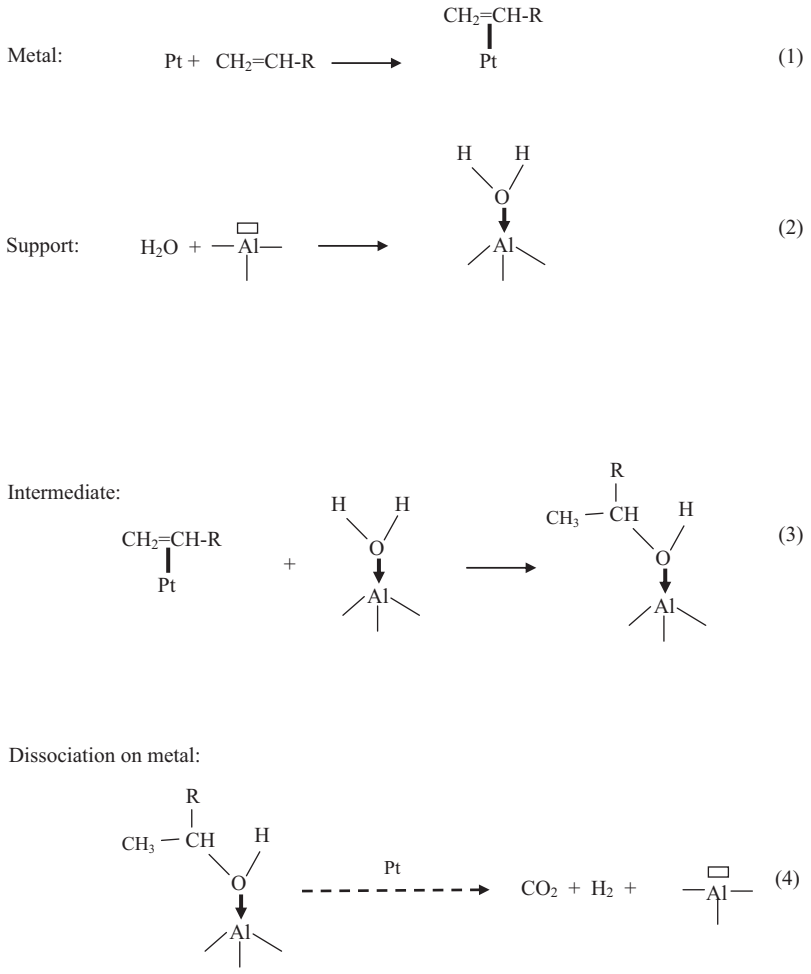

Fig. 6. Mechanism of steam reforming reaction occurring on the catalyst.

$Pt/\gamma\text{-}Al_2O_3$ for the conversion of n-butanol toward butanal. According to the results published by Papefthimiou et al., the opposite result could be expected since $Pt/\gamma\text{-}Al_2O_3$ presents a smaller average particle size (Fig. 1) [1]. Therefore, it seems reasonable to assign the higher activity of Pt/Al_2O_3-one-pot to its higher number of basic hydroxyls groups (Fig. 2).

For both catalysts a deceleration of the product formation occurs around 100–120 °C (Fig. 8(b) and Fig. 8(c)). This deceleration is detected while the proportion of n-butanol at the outlet is increasing (Fig. 8(a)). Two assumptions can be formulated to explain this phenomenon:

(i) an adsorption of a high amount of butanol on the catalyst and a low reaction rate leading to a reversible coking of the catalyst.
(ii) a high temperature and a low reaction rate leading to a desorption of n-butanol before its oxidation

Fig. 8(d) shows a deficit in carbon balance around 150–180 °C due to a reversible adsorption of carbonaceous species on

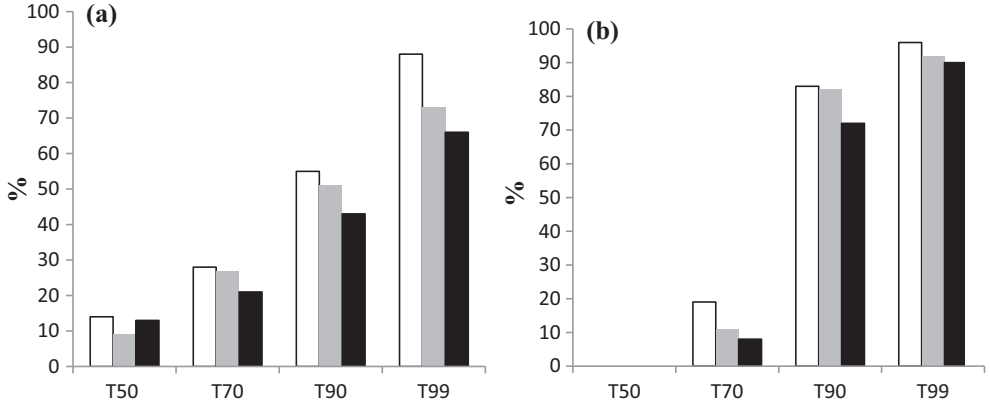

Fig. 7. Selectivity to CO_2 for different conversions of n-butanol (T_x: temperature for a n-butanol conversion = x) over (a) $\gamma\text{-}Al_2O_3$ and (b) $Pt/\gamma\text{-}Al_2O_3$ in presence of 0% (□), 3% (▒) and 10% (■) of water.

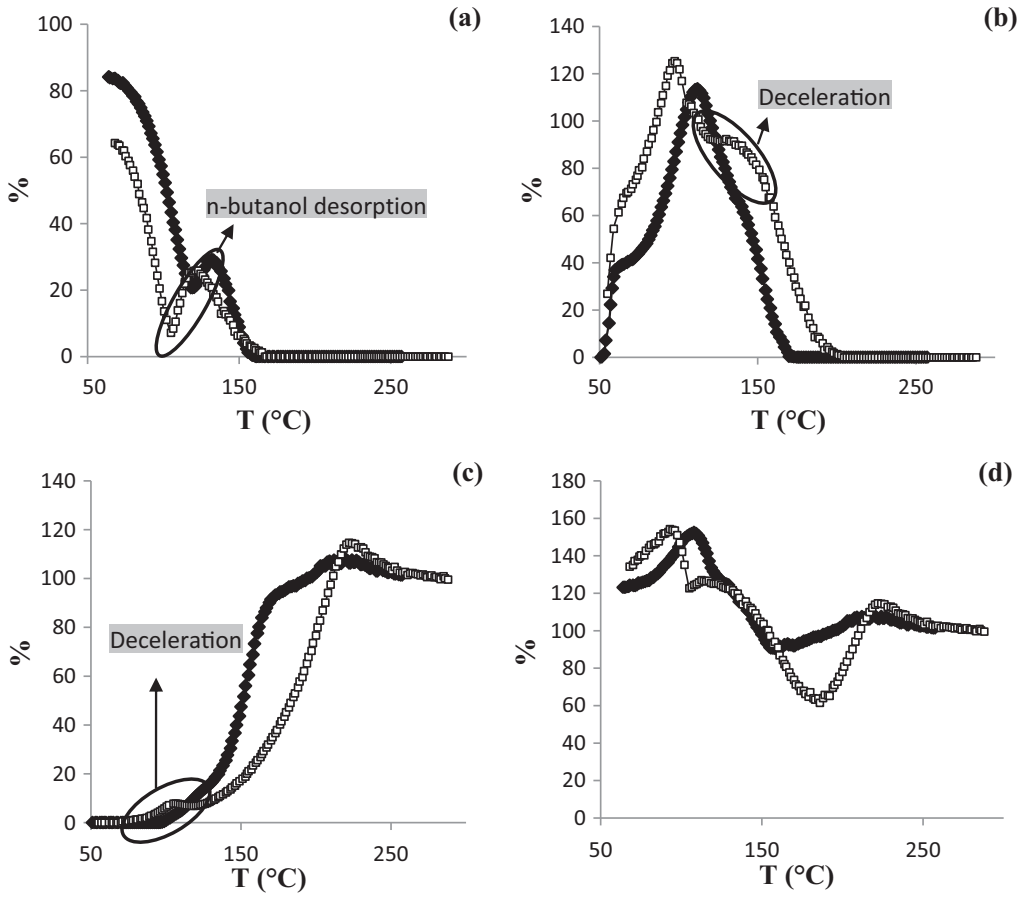

Fig. 8. Results obtained from the oxidation of n-butanol over (■) Pt/γ-Al_2O_3 and (◊) Pt/Al_2O_3-one-pot: (a) n-butanol, (b) butanal, (c) carbon dioxide and (d) carbon balance.

the catalyst surface. This phenomenon is more pronounced on Pt/Al_2O_3-one-pot due to its higher surface area and/or higher amount of total LAS. In consequence, the transformation of butanal to carbon dioxide is then limited on this catalyst (Fig. 8(c)). Thus, Pt/γ-Al_2O_3 presents better catalytic properties for total oxidation of n-butanol.

4. Conclusion

This study was focused on the catalytic removal of n-butanol. Platinum catalysts supported on alumina were prepared by incipient wetness impregnation and sol–gel methods. The objective was to evidence a relation between the acid–base properties and the catalyst reactivity. The acid–base properties of the catalysts were investigated by a FTIR study. An increase in the catalyst acidity leads to an enhancement of its activity in n-butanol dehydration and 1-butene isomerization. The n-butanol dehydrogenation is linked to the catalyst surface basicity in absence of platinum. The presence of oxygen suppresses n-butanol dehydration and promotes the dehydrogenation via an oxidative mechanism. N-butanol total oxidation depends on the ability of the catalyst to transform n-butanol into butanal and further butanal into carbon dioxide. The adsorption–desorption of reactants and products is the key factor in this oxidation and the limiting step seems to be desorption. An excessive amount of Lewis acid sites contributes to a deactivation of the catalyst by allowing the adsorption of a large proportion of carbonaceous species. Finally, this study demonstrates the inhibiting effect of water on n-butanol oxidation.

References

[1] P. Papaefthimiou, T. Ioannides, X.E. Verykios, Applied Catalysis B 13 (1997) 175–184.
[2] A. Janbey, W. Clark, E. Noordally, S. Grimes, S. Tahir, Chemosphere 52 (2003) 1041–1046.
[3] P. Papaefthimiou, T. Ioannides, X.E. Verykios, Catalysis Today 54 (1999) 81–92.
[4] L.F. Liotta, Applied Catalysis B 100 (2010) 403–412.
[5] P. Marécot, A. Fakche, B. Kellali, G. Mabilon, M. Prigent, J. Barbier, Applied Catalysis B (1994) 283–294.
[6] M.J. Patterson, D.E. Angove, N.W. Cant, Applied Catalysis B 26 (2000) 47–57.
[7] S.K. Agarwal, J.J. Spivey, J.B. Butt, Applied Catalysis A 81 (1992) 239–255.
[8] K.T. Chuang, S. Cheng, S. Tong, Industrial and Engineering Chemistry Research 31 (1992) 2466–2472.
[9] W.L. Holstein, C.J. Machiels, Journal of Catalysis 162 (1996) 118–124.
[10] L. van de Beld, M.P.G. Bijl, A. Reinders, B. van der Werf, K.R. Westerterp, Chemical Engineering Science 49 (1994) 4361–4373.
[11] S.F. Tahir, C.A. Koh, Chemosphere 38 (1999) 2109–2116.
[12] Z. Vit, J. Vala, J. Malek, Applied Catalysis 7 (1983) 159–168.
[13] P. Berteau, S. Ceckiewizc, B. Delmon, Applied Catalysis 31 (1987) 361–383.
[14] J.B. Peri, Journal of Physical Chemistry 69 (1965) 220–230.
[15] H. Knözinger, P. Ratnasamy, Catalysis Reviews: Science and Engineering 17 (1978) 31–70.
[16] J. Medema, J.J.G.M. van Bokhoven, A.E.T. Kuiper, Journal of Catalysis 25 (1972) 238–244.
[17] D.S. Mac Iver, H.H. Tobin, R.T. Barth, Journal of Catalysis 2 (1963) 485–497.
[18] C. Morterra, A. Chiorino, G. Chiotti, E. Garrone, Journal of the Chemical Society, Faraday Transactions 1 (1979) 271–288.
[19] D.S. Mac Iver, W.H. Wilmot, J.M. Bridges, Journal of Catalysis 3 (1964) 502–511.
[20] M. Yamadaya, K. Shimomura, T. Kinoshita, H. Uchida, Kogyo Kagaku Zasshi 72 (1969) 1050–1065.
[21] C. Morterra, S. Coluccia, G. Chiotti, A. Zecchina, Zeitschrift fur Physikalische Chemie – Neue Folge 104 (1977) 275–290.
[22] R.R. Bailey, J.P. Wightman, Journal of Colloid and Interface Science 70 (1979) 112–123.
[23] V.C.F. Holm, R.W. Blue, Industrial and Engineering Chemistry 43 (1951) 501–505.

[24] S.G. Hindin, S.W. Weller, Advances in Catalysis 9 (1957) 70–75.
[25] Y. Trambouze, L. de Mourges, M. Perrin, Journal de Chimie Physique 51 (1954) 723–728.
[26] J.B. Peri, Actes 2e Congr Intern Catalyse, vol. 1, Paris, 1960, 1961, pp. 1333–1352.
[27] Z.-X. Li, F.-B. Shi, L.-L. Li, T. Zhang, C.-H. Yan, Physical Chemistry Chemical Physics 13 (2011) 2488–2491.
[28] A.A. Tsyganenko, V.N. Filimonov, Spectroscopy Letters 5 (1972) 477–487.
[29] M. Digne, P. Sautet, P. Raybaud, P. Euzen, H. Toulhoat, Journal of Catalysis 226 (2004) 54–68.
[30] F. Abbattista, S. Delmastro, G. Gozzelino, D. Mazza, M. Vallino, G. Busca, V. Lorenzelli, G. Ramis, Journal of Catalysis 117 (1989) 42–51.
[31] C. Morterra, G. Magnacca, Catalysis Today 27 (1996) 497–532.
[32] S. Khabtou, T. Chevreau, J.-C. Lavalley, Microporous Materials 3 (1994) 133–148.
[33] F. Can, A. Travert, V. Ruaux, J.-P. Gilson, F. Maugé, R. Hu, R.F. Wormsbecher, Journal of Catalysis 249 (2007) 79–92.
[34] J. Hermia, S. Vigneron, Catalysis Today 17 (1993) 349–358.
[35] K.D. Rendulic, B.A. Sexton, Journal of Catalysis 78 (1982) 126–135.
[36] A.J. Van Roosmalen, M.C.G. Hartmann, J.C. Mol, Journal of Catalysis 66 (1980) 112–120.
[37] D. Ballivet, D. Barthomeuf, Y. Trambouze, Journal of Catalysis 35 (1974) 359–362.
[38] Z. Abbasi, M. Haghighi, E. Fatehifar, S. Saedy, Journal of Hazardous Materials 186 (2011) 1445–1454.
[39] D.C. Grenoble, Journal of Catalysis 51 (1978) 203–211.
[40] D. Duprez, P. Pereira, M. Grand, R. Maurel, Journal of Catalysis 75 (1982) 151–163.